Published in final edited form as:
Clin Cancer Res. 2012 October 15; 18(20): 5628–5638. doi:10.1158/1078-0432.CCR-12-1911.

Intracerebral CpG Immunotherapy with Carbon Nanotubes Abrogates Growth of Subcutaneous Melanomas in Mice

Haitao Fan[1,*], **Ian Zhang**[2,*], **Xuebo Chen**[3], **Leying Zhang**[2], **Huaqing Wang**[1], **Anna Da Fonseca**[4], **Edwin R. Manuel**[5], **Don J. Diamond**[5], **Andrew Raubitschek**[6], and **Behnam Badie**[2,6]

[1]Department of Neurosurgery, Provincial Hospital Affiliated to Shandong University, Jinan, P.R.China

[2]Division of Neurosurgery, City of Hope Beckman Research Institute, Duarte, California 91010

[3]Department of General Surgery, The Second Hospital of Jilin University, Changchun, Jilin Province, P.R. China

[4]Laboratório de Morfogênese Celular, Instituto de Ciências Biomédicas, Universidade Federal do Rio de Janeiro, Rio de Janeiro, Brazil, Bolsista do CNPq

[5]Division of Translational Vaccine Research, Department of Virology, City of Hope Beckman Research Institute, Duarte, California 91010

[6]Department of Cancer Immunotherapeutics & Tumor Immunology, City of Hope Beckman Research Institute, Duarte, California 91010

Abstract

Purpose—Recently, we showed that intratumoral delivery of low-dose, immunostimulatory CpG oligodeoxynucleotides conjugated with carbon nanotubes (CNT-CpG) was more effective than free CpG and not only eradicated intracranial (i.c.) gliomas, but also induced antitumor immunity that protected mice from subsequent i.c. or systemic tumor rechallenge. Here, we examined if the same "intracerebral immunotherapy" strategy could be applied to the treatment of metastatic brain tumors.

Experimental Design—Mice with both i.c. and subcutaneous (s.c.) melanomas were injected intratumorally with CNT-CpG into either location. Antitumor responses were assessed by flow cytometry, bioluminescent imaging, and animal survival.

Results—When given s.c., CNT-CpG response was mostly local, and it only modestly inhibited the growth of i.c. melanomas. However, i.c. CNT-CpG abrogated the growth of not only brain, but also s.c. tumors. Furthermore, compared to s.c. injections, i.c. CNT-CpG elicited a stronger inflammatory response that resulted in more potent antitumor cytotoxicity and improved *in vivo* trafficking of effector cells into both i.c. and s.c. tumors. To investigate factors that accounted for these observations, CNT-CpG biodistribution and cellular inflammatory responses were examined in both tumor locations. Intracranial melanomas retained the CNT-CpG particles longer and were infiltrated by TLR-9-positive microglia. In contrast, myeloid-derived suppressive cells were more abundant in s.c. tumors. Although depletion of these cells prior to s.c. CNT-CpG therapy enhanced its cytotoxic responses, antitumor responses to brain melanomas were unchanged.

Corresponding Author: Behnam Badie, Professor, Division of Neurosurgery, 1500 East Duarte Road, Duarte, CA 91010, Phone: 626-471-7100, Fax: 626-471-7344, bbadie@coh.org.
*These authors contributed equally to this project.

Conflicts of Interest: None

Conclusions—These findings suggest that intracerebral CNT-CpG immunotherapy is more effective than systemic therapy in generating antitumor responses that target both brain and systemic melanomas.

Keywords

Brain neoplasm; immunotherapy; immune-privilege; nanoparticle; toll-like receptor-9

Introduction

The brain is a common location for tumor metastasis; approximately one third of patients with systemic cancer ultimately develop central nervous system (CNS) involvement (1). This is due in part to the blood-brain barrier and the brain's "immune-privileged" status that, respectively, prevent the penetration of chemotherapeutic drugs and inflammatory cells into the CNS (1). Recent work however, has demonstrated that CNS immunosurveillance does indeed take place under both healthy and inflammatory conditions (2). In experimental gliomas, for example, activated T cells have the ability to find their targets in the brain (3). These observations have prompted the development of vaccine therapies against brain tumors (4). However, despite induction of an effective systemic immunity, the immunosuppressive microenvironment of the tumor itself may attenuate the host antitumor responses.

Local immunosuppressive tumor milieu, caused by low levels of MHC class I expression, production of immunosuppressive factors, and scarcity of antigen presenting cells have all been considered to account for the poor immune responsiveness of brain tumors (5). One strategy to overcome these local barriers is through activation of the innate immune system. Cells that comprise this system, including microglia (MG), macrophages (MP), monocytes, NK and dendritic cells (DC), express pattern-recognition receptors which collectively recognize macromolecules that are broadly expressed by micro-organisms. Among these, activation of toll-like receptors (TLRs) has been shown to enhance phagocytosis, promote secretion of Th1 cytokines, and mediate leukocyte recruitment to infected tissues (6–8). Consequently, agonists such as CpG oligodeoxynucleotides (CpG) that bind TLR9 have been evaluated as cancer vaccine adjuvants and have shown some efficacy in inducing adaptive and antigen-specific, cellular antitumor immune responses in animal models (9). However, early-stage clinical trials in patients with melanoma and gliomas have been less promising (6, 10–11). Furthermore, high doses of CpG may exacerbate brain edema when directly injected into brain tumors. Because TLR9 is located on endosomes, we hypothesized that poor CpG uptake by tumor-associated inflammatory cells may account for the weak clinical responses and therefore, evaluated nanoparticles to improve the delivery of CpG into brain tumors.

To enhance CpG activity, functionalized carbon nanotubes (CNTs) were conjugated with CpG (CNT-CpG) and tested in glioma-bearing mice (12). The CNTs not only enhanced CpG uptake by tumor-associated leukocytes, but also resulted in the eradication of intracranial (i.c.) gliomas, even at low doses (12). Interestingly, surviving animals also exhibited a durable tumor-free remission and were protected from tumor rechallenge, suggesting induction of systemic antitumor immunity. These findings suggested that i.c. CpG therapy with a CNT delivery system could potentially be used for the treatment of systemic immunogenic tumors with brain metastasis. Here, we tested this hypothesis and surprisingly noted that intracerebral CNT-CpG immunotherapy is superior to systemic therapy in generating antitumor responses. These studies also identified CNS-specific microenvironmental factors that may enhance immune responses to CNT-CpG.

Materials and Methods

Reagents

Thiolated CpG (5′-TGACTGTAACGTTCGAGATGA-3′) was constructed as described by Rosi *et al.* (13) and labeled with Cy5.5 (Lumiprobe, LLC). All flow mAb ((i.e. CD11b, CD45, CD11c, CD8, NK1.1, Ly-6G (clone RB6-8c5) and Ly-6C (clone HK1.4)) and isotype controls were purchased from BD Biosciences (San Jose, CA) or eBiosciences (San Diego, CA).

Cell lines

B16.F10 melanoma cell line of C57BL/6 origin was purchased from ATCC in 2011 and stably transfected with firefly luciferase expression vector. Positive clones (B16.F10-luc) were selected using zeocin (1 mg/mL) and G418 and cultured in DMEM supplemented with 10% fetal bovine serum, penicillin (100 units/mL), and streptomycin (100 μg/mL) at 37°C in a humidified 5% CO2 atmosphere. Tumorigenicity of the B16.F10-luc cells was authenticated by histological characterization of melanomas generated in mice.

Single-walled CNT construction and functionalization

Single-walled CNTs measuring 200–400nm in length were generated and characterized by electron microscopy as previously described (12). CNT functionalization was performed using methods described by Liu *et al.* (14–15). Briefly, hipco CNTs were sonicated extensively (1 hour) in a solution of 1, 2-Distearoyl-Sn-Glycero-3-Phosphoethanolamine-N-[Amino (Polyethylene Glycol) 2000] (PEG) (Avanti Polar Lipids, Alabama). The supernatant solution of PEG-CNT was collected after centrifuge at 24,000*g* for 6 hours. After removal of excess PEG molecules with an Amicon centrifugal filter unit (100 kDa), functionalized PEG-CNTs were conjugated with Sulfo-LC-SPDP (Thermo Fisher Scientific Inc., USA) for 1 hour at RT. After removal of excess Sulfo-LC-SPDP with an Amicon centrifugal filter unit (100 kDa) (Millipore, Billerica, Massachusetts), the CNT conjugates were quantified using a SpectraMax M2 (Sunnyvale, California, USA) spectrometer with a weight extinction coefficient of 0.0465 l mg^{-1} cm^{-1} at 808 nm. CNTs were then conjugated with CpG through a cleavable disulfide bond at 4°C for 24 hours. Free CpG was then separated from solution using an Amicon centrifugal filter unit (100 kDa) (Millipore, Billerica, Massachusetts) and measured using a NanoDrop 1000 Spectrophotometer (Thermo Scientific). CNT-bound CpG was quantified by subtracting the unbound CpG from total CpG added prior to the conjugation reaction.

In vitro NF-κB assay

RAW MP cells (RAW-Blue™) stably transfected with a reporter construct expressing a secreted embryonic alkaline phosphatase gene under the control of a promoter inducible by the transcription factors NF-κB and AP-1 (InvivoGen) were used to measure TLR9 activation. Upon TLR stimulation, RAW-Blue™ cells induce the activation of NF-κB and AP-1, and subsequently the secretion of quantifiable secreted embryonic alkaline phosphatase.

Tumor implantation, treatment, and imaging

All animals were housed and handled in accordance to the guidelines of City of Hope Institutional Animal Care and Use Committee (IACUC). Intracranial tumor implantation was performed stereotactically at a depth of 3 mm through a bur hole placed 2mm lateral and 0.5 mm anterior to the bregma as previously described (16). B16.F10-luc cells were harvested by trypsinization, counted, and resuspended in PBS. Female C57BL/6 mice (Jackson Laboratory, Bar Harbor, ME) weighing 15–25 g were anesthetized by

intraperitoneal administration of ketamine (132 mg/kg) and xylazine (8.8 mg/kg), and immobilized in a stereotactic head frame. Intracranial tumors implantation was performed by injecting 3 μl of PBS containing 5×10^3 tumor cells through a small burr hole. Subcutaneous (s.c.) tumors were generated by injecting 100 μl of PBS containing 10^5 tumor cells.

Four days after i.c. and s.c. tumor implantation, mice received intratumoral (i.t.) injections of PBS (control, 10 μl), free CpG (5 μg/10 μl PBS), PL-PEG-functionalized blank CNT (2.5 μg), and CpG conjugated to CNT (CNT-CpG; 2.5 μg CNT/5 μg CpG/10 μl PBS) at the same stereotactic coordinates used for tumor implantation. Depending on the experimental design, 1–3 injections were given every 3–4 days. Tumor growth was assessed by a Xenogen IVIS *In Vivo* Imaging System (Xenogen, Palo Alto, CA) as previously described (12).

In vivo uptake and distribution studies

Mice bearing i.c. tumors were injected i.t. with CNT bound to Cy5.5-labeled CpG (CNT-$CpG^{5.5}$, 2.5 μg CNT/5 μg CpG/10 μl PBS) or free $CpG^{5.5}$ (5 μg CpG/10 μl PBS). I*n vivo* Cy5.5 signal was measured with a Xenogen IVIS Imaging System. For direct imaging, tumors were harvested at various time intervals, frozen, embedded in O.C.T. (Tissue-Tek), and 10 μm sections were cut using a cryostat (Leica Microsystem Inc., Bannockburn, IL). Sections were mounted in Vectashield mounting medium containing 4060-diamidino-2-phenylindole (DAPI) (Vector, Burlingame, CA). Images were obtained by Nikon Eclipse 80i microscope (Nikon Japan) and were prepared by Metamorph imaging software.

Chromium release cytotoxicity assay

Cytotoxicity against B16.F10 melanoma cells was determined using a standard ^{51}Cr release assay (17). Briefly, effector cells were derived from spleens of B16.F10-bearing C57BL6 mice (n=4) treated with either i.c. or s.c. CNT-CpG. CNT-CpG injections were given three times, four days after initial tumor implantation and every subsequent 3 days. Mice were sacrificed 48 hours after the final treatment and splenocytes (effectors) were harvested and co-incubated with irradiated (30,000 rad) B16.F10 cells for 7 days. Effectors were then co-incubated for 6 hours with 5,000 Cr^{51}-loaded B16.F10 targets in 96-well plates at ratios of 100:1, 20:1, and 4:1 (in triplicate). Radioactivity released into the supernatant was measured using a Cobra Quantum gamma counter (PerkinElmer). Percent specific lysis was calculated as: (experimental release -spontaneous release)/(maximum release - spontaneous release) × 100%.

Flow cytometry analysis

Tumors were harvested and examined by flow cytometry as previously described (12). Cell suspensions from brain and s.c. tissue were forced through a 40 μm filter. Freshly-prepared samples were resuspended in 0.1 M PBS containing 1% FBS and 2 mM EDTA and incubated with FcγIII/IIR-specific Ab to block nonspecific binding. Samples were then stained with different combinations of mAb or isotype controls for 1 hour at 4°C and analyzed by a CyAn fluorescence cell sorter (BDIS, San Jose, CA). Inflammatory cells were gated and separated from the remainder of the sorted cells based on forward vs. side-scatter analysis and staining characteristics. FlowJo 8.4.7 software (Tree Star, Inc., Ashland, OR) was used for data analysis and the proportion of each cell type was measured as percent of total inflammatory cells. Tumor MPs were gated as $CD45^{high}$ $CD11b^+$ and MG as $CD45^{low}$ $CD11b^+$, based on a previously described phenotypic characterization (18). *In vivo* TLR9 staining was carried out by using Fixation/Permeabilization solution according to the manufacturer's instructions (BD Pharmingen, San Diego, CA).

In vivo leukocyte trafficking

Mice bearing either i.c. or s.c. tumors (n=3/group) were given three injections of i.t. CNT-CpG four days after initial tumor implantation and every subsequent 3 days. Splenocytes were isolated 24 hours later the third injection and incubated with CFSE (5mM) for 5 minutes and then washed with 10 ml of medium containing 5% FBS. Labeled cells were re-injected through the tail vein into untreated recipient mice (1×10^8 cells/mouse) that had been implanted with i.c. and s.c. melanomas 10 days earlier (n=5/group). Tumors were harvested 24 hours later and tested for presence of CFSE-labeled NK and CD8 cells by flow cytometry.

NK, CD8 and Gr-1 depletion

NK and CD8 depletion studies were carried out as described previously (12). In these experiments, mice were injected with anti-CD8, anti-NK1.1, or control IgG (200 μg/mouse, i.p.) mAb one day prior to tumor implantation and each i.t. CNT-CpG injection. Leukocyte depletion was confirmed with FACS analysis of peripheral blood (12). For Gr-1 depletion studies, the RB6-8C5 hybridoma (originally produced by Robert L. Coffman) was used to generate the Gr-1 mAb (against Ly6C) and was a kind gift from Dr. Hans Schreiber. The hybridoma was maintained in RPMI containing 10% FBS. To assess the role of MDSCs on CNT-CpG therapy, mice were treated with anti-Gr-1 mAb or control IgG (30 mg/mouse) one day prior and every 3 days after tumor implantation (a total of 5 injections). Animals were then implanted with both i.c. and s.c. tumors and then treated with i.t. PBS or CNT-CpG four, seven and ten days later.

Statistical analysis

Statistical comparison in all different experimental conditions was performed with the prism software using two-way analysis of variance (ANOVA) or the Student's t-test. Survival was plotted using a Kaplan-Meir survival curve and statistical significance was determined by the Log-rank (Mantel-Cox) test. A P value of less than 0.05 was considered significant.

Results

CNT-CpG antitumor response

To control for variations in CNT-CpG preparations, CNT-CpG-mediated TLR9 activation was examined using an *in vitro* NF-κB assay prior to *in vivo* testing (Suppl. Fig. 1). Only those CNT-CpG preparations that increased NF-κB activity at least 2-fold over an equivalent dose of free CpG at 24 hours were selected for animal studies. In our experience, CNT-CpG preparations with less activity have not shown significant antitumor response in this model (unpublished data).

To confirm if i.c. CNT-CpG elicited a systemic antitumor response, mice with both i.c. and s.c. B16.F10-luc melanomas were treated twice i.c. with CNT-CpG, or with CNTs that were functionalized only with PL-PEG and do not have any tumoricidal effect (12, 19). When administered i.c., CNT-CpG inhibited the growth of not only i.c., but also s.c. melanomas (Fig. 1). To test if this antitumor effect was specific for CNT delivery, a group of mice were treated i.c. with free CpG in a similar experiment (Suppl. Fig. 2). At these low doses (i.e. (5 μg), i.c. CpG had no effect on i.c. tumors, but it did inhibit s.c. tumor growth, although not as much as CNT-CpG (Suppl. Fig. 2A). Furthermore, i.c. CNT-CpG antitumor responses were mediated by both CD8 and NK cells (Suppl. Fig. 2B), similar to our observations in i.c. gliomas (12). These findings suggested that low doses of i.c. CNT-CpG was able to generate not only a local, but also a systemic antitumor response. However, unlike glioma models where 60% of tumors were completely eradicated by i.c. CNT-CpG, melanoma-bearing mice were not cured by this treatment (Suppl. Fig. 2B). To further evaluate the impact of

tumor microenvironment on CNT-CpG efficacy, a similar experiment was performed except that animals were treated with either i.c. or s.c. CNT-CpG (Fig. 2). As before, untreated mice died within two weeks of tumor implantation from CNS disease (not shown), and i.c. CNT-CpG inhibited the growth of both i.c. and s.c. melanomas (Fig. 2A and B). Of note, development of this systemic immune response required tumor presence in the CNS, as mice that lacked i.c. melanomas did not exhibit antitumor activity against s.c. tumors (Fig. 2B). Unlike i.c. therapy, s.c. CNT-CpG response was mostly local (Fig. 2B), and not as effective in controlling the growth of i.c. melanomas (Fig. 2A and C). These observations suggested that the stronger antitumor efficacy of i.c. CNT-CpG was due to either better CNS trafficking of cytotoxic cells caused by blood-brain barrier disruption, or CNS-specific micro-environmental factors that enhanced immune responses to CNT-CpG. To test these possibilities, we next assessed the inflammatory responses to CNT-CpG therapy in both tumor locations.

Role of tumor location on CNT-CpG inflammatory responses

To investigate cellular responses to CNT-CpG therapy, mice bearing 4 day-old i.c. and s.c. B16.F10 melanomas received i.t. PBS or CNT-CpG and tumor inflammatory cells were analyzed by FACS after 24 hours (Fig. 3). Treatment with i.c. CNT-CpG increased the infiltration of MP ($CD45^{hi}$ $CD11b^{+}$), NK, CD8, and CD4 cells into brain tumors (Fig. 3A), but had no effect on inflammatory cell infiltration into the untreated s.c. tumors in the same animals (Fig. 3B). After CNT-CpG treatment, MG ($CD45^{low}$ $CD11b^{+}$) in i.c. tumors decreased in proportion to other leukocytes as a result of influx of other inflammatory cells (Fig. 3A). In contrast to i.c. injections, s.c. CNT-CpG treatment promoted MP ($CD11b^{+}$), and to a lesser extent, NK infiltration; CD8 and CD4 influx were not significantly affected (Fig. 3B). Therefore, i.c. CNT-CpG appeared to induce a stronger local inflammatory reaction in tumors compared to s.c. injections. To test if the local cellular responses to CNT-CpG correlated with systemic antitumor activity, splenocytes from the treated animals were harvested and tested for tumor cytotoxicity. Interestingly, effector cells from i.c. CNT-CpG-injected mice elicited a stronger *ex vivo* antitumor response when compared to s.c.-treated tumors (Fig. 3C). To evaluate leukocyte trafficking, splenocytes from mice bearing either brain or s.c. tumors that were treated with i.t. CNT-CpG were isolated and re-injected into untreated recipient mice with both i.c. and s.c. tumors. Interestingly, when compared to s.c. treatment, NK and CD8 cells that were isolated from i.c.-treated mice appeared to have improved trafficking into both i.c. and s.c. tumors that had not been treated with CNT-CpG (Fig. 3D). These observations suggested that CNS microenvironmental factors enhanced both antitumor responses and trafficking of effector cells generated by intracerebral CNT-CpG.

CNT-CpG distribubion

To study the role of tumor location on CNT-CpG distribution, mice with both i.c. and s.c. melanomas were injected i.t. with free $CpG^{5.5}$ or CNT-$CpG^{5.5}$. Tumor growth and Cy5.5 signal were then monitored by Xenogen imaging (Fig. 4A). Although both CpG and CNT-CpG were completely cleared from s.c. tumors (Fig 4B), some Cy5.5 signal was still detectable in i.c. tumors even after 7 days of injections (Fig. 4C). Also, conjugation of CpG to CNT did not appear to change its clearance from tumors. Because the antitumor activity of free CpG was weaker than CNT-CpG (Suppl. Fig. 2), we next compared the regional distribution of free CpG to CNT-CpG in i.c. melanomas (Fig. 4D). Within a few days, free CpG appeared to diffuse away from the injection site, while CNT-CpG particles dispersed around the tumor margin. Therefore, even though the overall free $CpG^{5.5}$ signal intensity was similar to CNT-$CpG^{5.5}$, its distribution around i.c. tumors was different, possibly due to uptake of CNT-CpG complexes by tumor-associated leukocytes and their migration around tumor periphery (12, 19). To further study the role of tumor microenvironment on CNT-

CpG response, we next evaluated the expression of TLR9 (CpG receptor) by tumor-associated inflammatory cells.

TLR9 expression

We previously showed that inflammatory cells (notably MG, MP, and NK cells) are the main carriers of CNT-CpG particles in experimental gliomas (12, 19). To further characterize microenvironmental differences that may have accounted for CNT-CpG antitumor responses, we studied the expression of TLR9 in tumor-associated leukocytes in i.c. and s.c. melanomas (Fig. 5). Microglia were the most frequent inflammatory cells in newly-implanted untreated i.c. tumors (50–60%) and accounted for most of the TLR9-positive cells. However, infiltrating NK and CD11c (dendritic) cells (not shown), which accounted for less than 10% of tumor leukocytes, also expressed TLR9. In s.c. melanomas, MP, NK and CD11c cells each accounted for less than 10% of tumor-associated inflammatory cells but equally expressed TLR9. Also, concurrent growth of i.c. and s.c. tumors in the same animal did not significantly influence TLR9 expression in newly-implanted tumors.

Because $CD11b^+$ cells markedly increased in i.c. and s.c. tumors after CNT-CpG therapy (Fig. 3A and B), and because these cells are comprised of a heterogeneous cell population, we next characterized the impact of tumor microenvironment on $CD11b^+$ phenotypes (Fig. 6). At baseline, the proportion of infiltrating MPs with myeloid-derived suppressive cell phenotype (MDSC, $Gr\text{-}1^+$) was very low in early-stage i.c. tumors (Fig. 6A). After CNT-CpG injection, however, both $Ly6C^+$ and $Ly6G^+$ cells equally increased in the injected i.c. tumors. In s.c. tumors, however, $Gr\text{-}1^+$ cells were more prevalent at baseline and significantly increased after CNT-CpG treatment (Fig. 6B). Interestingly, the proportion of monocytic MDSC (M-MDSC; $Ly6C^{high}$) was higher than granulocytic MDSC (G-MDSC, $Ly6G^+$ $Ly6C^{low}$) in the CNT-CpG-treated s.c. tumors. Although both cell types are considered to be MDSCs, M-MDSC have a higher tumor suppressive activity in mice (20). To test if MDSCs in s.c. tumors played a role in weaker antitumor responses, these cells were depleted prior to CNT-CpG therapy.

Gr-1 depletion

To assess the role of MDSCs on CNT-CpG therapy, mice were treated with either anti-Gr-1 mAb or control IgG prior to tumor implantation and CNT-CpG therapy. Analysis of tumors two days after the final CNT-CpG treatment demonstrated a decrease in tumor-infiltrating M-MDSCs (but an increase in G-MDSC) in s.c. tumors (suppl. Fig. 3). Interesting, alterations in MDSC profile with anti-Gr-1 mAb enhanced the antitumor cytotoxicity of effector cells isolated from s.c., but not i.c. CNT-CpG-treated animals (Fig. 6C). Despite an increase in *ex vivo* cytotoxicity, however, *in vivo* antitumor response against i.c. melanomas remained the same and s.c. CNT-CpG-treated animals had similar survival even after Gr-1 depletion (Fig. 6D). These findings suggest that although infiltration of MDSCs may have partially abrogated the immunostimulatory functions of CNT-CpG, effector cell trafficking into i.c. tumors may have still limited the remote antitumor efficacy of cytotoxic cells that were primed in the s.c. tumors.

Discussion

Immunotherapy is an attractive treatment modality for immunogenic tumors such as melanomas. Although various approaches for melanoma immunotherapy have been pursued with mixed results, recent findings from a phase III randomized trial of CTLA-1 blocking agent has validated the efficacy of this approach (21). One limitation for effective melanoma immunotherapy, however, may be the high frequency of brain metastasis which occurs in

10–70% of patients (22–23). Although activated T cells can penetrate i.c. tumors, clinical studies have demonstrated that less than 50% of CNS metastases respond to systemic adoptive immunotherapy in melanoma patients (24). Therefore, there is a need for improved immune-targeting of metastatic brain tumors. Recently, while examining the role of CpG immunotherapy with nanoparticles, we observed a systemic antitumor response in experimental gliomas (12). Here, we have confirmed these findings in a melanoma model by demonstrating that i.c. CNT-CpG inhibited the growth of both brain and s.c. melanomas. To our knowledge, these results have not been previously reported and they suggest that intracerebral CNT-CpG therapy may have utility for the treatment of not only of gliomas, but also metastatic brain tumors.

Brain has been considered to be an “immune privileged” organ. Tumors that are spontaneously rejected when implanted into the s.c. tissue can propagate in the CNS of immunocompetent hosts (25). Furthermore, systemic implantation of some tumors can generate effective memory T cell responses that are capable of rejecting tumors in the brain (25). In fact, this phenomenon (which has been partly attributed to local immunosuppressive brain microenvironment) is being exploited to develop vaccines against malignant gliomas. Here, however, we demonstrate that when stimulated with CNT-CpG, the “immune privileged” status of the brain can be reversed, resulting in the generation of anti-tumor immune responses that may even be superior to systemic stimulation. Our findings, while counterintuitive, highlight unique CNS factors that may be important in potentiating immune responses to CNT-CpG therapy.

Besides direct intracerebral injection of pro-inflammatory molecules such as CpG, other approaches have been attempted to enhance local CNS immune responses against i.c. tumors. Brain immune privilege could be overcome through exogenous expression of fms-like tyrosine kinase ligand 3, which resulted in DC recruitment and antigen presentation (26). Others have shown improvement in antitumor responses to DC vaccine when the cells were also given locally into the brain (27). In particular, Yamanaka *et al.* found improved survival of patients with recurrent gliomas when they received i.t. DC vaccines in addition to intradermal administration (28). Although the value of i.c. vaccine approaches to enhance systemic therapies against brain tumors has been suggested in these studies, the utility of this approach for immunotherapy of systemic tumors has not yet been reported.

In this study, we noted antitumor immune responses to be stronger when CNT-CpG was injected into i.c. tumors as compared to s.c. tumors. In contrast to s.c. CNT-CpG, which suppressed s.c. tumor growth but only had a modest inhibitory effect on i.c. melanomas, i.c. CNT-CpG abrogated the growth of both i.c. and s.c. tumors. Intracerebral administration of CNT-CpG also induced a stronger local inflammatory response and a more potent antitumor cytotoxicity, and improved trafficking of effector cells into tumors. These findings support the presence of unique CNS factors that potentiated CNT-CpG responses. Presence of TLR9-expressing MG cells, which are unique CNS MPs capable of phagocytosis and T cell activation, may have played a role in this process. These cells may have also accounted for delayed clearance of nanoparticles from the brain.

We previously showed functionalize CNTs to be non toxic and enhanced CpG immune responses in glioma models (12, 19). Although this immune activation may not be unique to the CNT delivery mechanism, and may also occur with other nanoparticles that promote CpG uptake into TLR9-containing endosomes, we noted several features that may be unique to the brain. First, distribution of CNT-CpG and CpG appeared to be different in i.c. tumors compared to s.c. melanomas. Although CNT-CpG and CpG completely cleared from s.c. tumors, some were retained in i.c. tumors even after a week of injection. Due to the potential for dissociation of Cy5.5 from CpG, and CpG from CNTs, this experiment may not have

exactly measured the biodistribution of CNT complexes. Based on previous studies with functionalized CNTs, we predict that the CNT complexes that are phagocytosed by tumor stroma to remain in the brain, while others are cleared by circulating monocytes before excretion by the biliary and renal pathways (19, 29). Nevertheless, our observations still highlighted unique CNS-specific factors that resulted in longer retention of both CNT-CpG and CpG in i.c. melanomas compared to s.c. tumors. Furthermore, the distribution of CNT-CpG around tumor margin was distinct from free CpG, which diffused throughout the injected hemisphere. Our previous studies have shown that local MG actively uptake CNT and CpG complexes (12). Because MG do not migrate out of the CNS, their retention and distribution around i.c. tumors may have accounted for the stronger antitumor responses with intracerebral CNT-CpG.

While evaluating of tumor-associated MP, we also noted differences in MDSC infiltration in each tumor location. Shortly after tumor implantation, MDSC infiltration was observed in s.c. tumors but not in i.c. melanomas. In contrast, most $CD11b^+$ cells in i.c. tumors were comprised of MG that did not express Gr-1. Even though both G-MDSC and M-MDSC increased after CNT-CpG injections in each tumor location, M-MDSC were more frequent in s.c. melanomas. On a per cell basis M-MDSC are considered to possess more suppressive activity than G-MDSC cells (20). Depletion of M-MDSC enhanced *ex vivo* antitumor effector activity, confirming that the influx of these cells into s.c. tumors may have muted immune responses to s.c. CNT-CpG. However, even after Gr-1 depletion, s.c. CNT-CpG failed to significantly inhibit the growth of i.c. tumors. These observations suggest that leukocyte trafficking into the brain may have ultimately determined the efficacy of CNT-CpG antitumor responses. Whereas CD8 and NK cells that were activated in the CNS were capable of migrating into both brain and s.c. tumors, effector cells that were primed in s.c. tumors may not have penetrated the CNS in sufficient numbers to effectively inhibit the growth of brain tumors.

In summary, we have verified the efficacy of a nanoparticle delivery system for optimizing CpG immunotherapy in a mouse melanoma model. More significantly, we have demonstrated potential value of intracerebral CNT-CpG for metastatic brain tumor therapy. Efficient uptake of CNT-CpG by tumor-associated MG in the brain, and their retention and wider distribution around tumors may have accounted for a stronger immune response following intracerebral CNT-CpG injections. In contrast to our glioma model, however, i.c. melanomas were not completely eradicated by i.t. CNT-CpG treatment in these experiments. Therefore, future studies will evaluate this approach in conjunction with other therapies such as cytotoxic T-lymphocyte-associated antigen 4 (CTLA-4) and death 1 protein (PD-1) inhibitors that have demonstrated efficacies as immune modulators.

Supplementary Material

Refer to Web version on PubMed Central for supplementary material.

Acknowledgments

The authors thank Dr. Harish Manohara (Jet Propulsion Laboratory, Pasadena, CA) for providing the carbon nanotubes, Dr. Piotr Swiderski (Department of Molecular Medicine) for generating thiolated CpG constructs.

Grant Support: This work was supported by R21CA131765, R01CA155769, James S. McDonnell Foundation (BB), ThinkCure Foundation (BB and DJD), and P01-CA030206 and CA077544 (DJD). The City of Hope Flow Cytometry Core was equipped in part through funding provided by ONR N00014-02-1 0958, DOD 1435-04-03GT-73134, and NSF DBI-9970143.

References

1. Steeg PS, Camphausen KA, Smith QR. Brain metastases as preventive and therapeutic targets. Nat Rev Cancer. 2011; 11:352–63. [PubMed: 21472002]
2. Galea I, Bechmann I, Perry VH. What is immune privilege (not)? Trends Immunol. 2007; 28:12–8. [PubMed: 17129764]
3. Prins RM, Shu CJ, Radu CG, Vo DD, Khan-Farooqi H, Soto H, et al. Anti-tumor activity and trafficking of self, tumor-specific T cells against tumors located in the brain. Cancer Immunol Immunother. 2008; 57:1279–89. [PubMed: 18253732]
4. Hickey MJ, Malone CC, Erickson KL, Jadus MR, Prins RM, Liau LM, et al. Cellular and vaccine therapeutic approaches for gliomas. J Transl Med. 2010; 8:100. [PubMed: 20946667]
5. Gomez GG, Kruse CA. Mechanisms of malignant glioma immune resistance and sources of immunosuppression. Gene Ther Mol Biol. 2006; 10:133–46. [PubMed: 16810329]
6. Carpentier A, Laigle-Donadey F, Zohar S, Capelle L, Behin A, Tibi A, et al. Phase 1 trial of a CpG oligodeoxynucleotide for patients with recurrent glioblastoma. Neuro Oncol. 2006; 8:60–6. [PubMed: 16443949]
7. Dalpke AH, Schafer MK, Frey M, Zimmermann S, Tebbe J, Weihe E, et al. Immunostimulatory CpG-DNA activates murine microglia. J Immunol. 2002; 168:4854–63. [PubMed: 11994434]
8. El Andaloussi A, Sonabend AM, Han Y, Lesniak MS. Stimulation of TLR9 with CpG ODN enhances apoptosis of glioma and prolongs the survival of mice with experimental brain tumors. Glia. 2006; 54:526–35. [PubMed: 16906541]
9. Jahrsdorfer B, Weiner GJ. CpG oligodeoxynucleotides as immunotherapy in cancer. Update Cancer Ther. 2008; 3:27–32. [PubMed: 19255607]
10. Weber JS, Zarour H, Redman B, Trefzer U, O'Day S, van den Eertwegh AJ, et al. Randomized phase 2/3 trial of CpG oligodeoxynucleotide PF-3512676 alone or with dacarbazine for patients with unresectable stage III and IV melanoma. Cancer. 2009; 115:3944–54. [PubMed: 19536884]
11. Carpentier A, Metellus P, Ursu R, Zohar S, Lafitte F, Barrie M, et al. Intracerebral administration of CpG oligonucleotide for patients with recurrent glioblastoma: a phase II study. Neuro Oncol. 2010; 12:401–8. [PubMed: 20308317]
12. Zhao D, Alizadeh D, Zhang L, Liu W, Farrukh O, Manuel E, et al. Carbon nanotubes enhance CpG uptake and potentiate antiglioma immunity. Clin Cancer Res. 2011; 17:771–82. [PubMed: 21088258]
13. Rosi NL, Giljohann DA, Thaxton CS, Lytton-Jean AK, Han MS, Mirkin CA. Oligonucleotide-modified gold nanoparticles for intracellular gene regulation. Science. 2006; 312:1027–30. [PubMed: 16709779]
14. Kateb B, Van Handel M, Zhang L, Bronikowski MJ, Manohara H, Badie B. Internalization of MWCNTs by microglia: possible application in immunotherapy of brain tumors. Neuroimage. 2007; 37 (Suppl 1):S9–17. [PubMed: 17601750]
15. Manohara HM, Wong EW, Schlecht E, Hunt BD, Siegel PH. Carbon nanotube Schottky diodes using Ti-Schottky and Pt-Ohmic contacts for high frequency applications. Nano Lett. 2005; 5:1469–74. [PubMed: 16178259]
16. Alizadeh D, Zhang L, Brown CE, Farrukh O, Jensen MC, Badie B. Induction of anti-glioma natural killer cell response following multiple low-dose intracerebral CpG therapy. Clin Cancer Res. 2010; 16:3399–408. [PubMed: 20570924]
17. Manuel ER, Blache CA, Paquette R, Kaltcheva TI, Ishizaki H, Ellenhorn JD, et al. Enhancement of cancer vaccine therapy by systemic delivery of a tumor-targeting Salmonella-based STAT3 shRNA suppresses the growth of established melanoma tumors. Cancer Res. 2011; 71:4183–91. [PubMed: 21527558]
18. Alizadeh D, Zhang L, Hwang J, Schluep T, Badie B. Tumor-associated macrophages are predominant carriers of cyclodextrin-based nanoparticles into gliomas. Nanomedicine. 2010; 6:382–90. [PubMed: 19836468]
19. VanHandel M, Alizadeh D, Zhang L, Kateb B, Bronikowski M, Manohara H, et al. Selective uptake of multi-walled carbon nanotubes by tumor macrophages in a murine glioma model. J Neuroimmunol. 2009; 208:3–9. [PubMed: 19181390]

20. Youn JI, Gabrilovich DI. The biology of myeloid-derived suppressor cells: the blessing and the curse of morphological and functional heterogeneity. Eur J Immunol. 2010; 40:2969–75. [PubMed: 21061430]
21. Hodi FS, O'Day SJ, McDermott DF, Weber RW, Sosman JA, Haanen JB, et al. Improved survival with ipilimumab in patients with metastatic melanoma. N Engl J Med. 2010; 363:711–23. [PubMed: 20525992]
22. Sampson JH, Carter JH Jr, Friedman AH, Seigler HF. Demographics, prognosis, and therapy in 702 patients with brain metastases from malignant melanoma. J Neurosurg. 1998; 88:11–20. [PubMed: 9420067]
23. de la Monte SM, Moore GW, Hutchins GM. Patterned distribution of metastases from malignant melanoma in humans. Cancer Res. 1983; 43:3427–33. [PubMed: 6850649]
24. Lonser RR, Song DK, Klapper J, Hagan M, Auh S, Kerr PB, et al. Surgical management of melanoma brain metastases in patients treated with immunotherapy. J Neurosurg. 2011; 115:30–6. [PubMed: 21476810]
25. Volovitz I, Marmor Y, Azulay M, Machlenkin A, Goldberger O, Mor F, et al. Split immunity: immune inhibition of rat gliomas by subcutaneous exposure to unmodified live tumor cells. J Immunol. 2011; 187:5452–62. [PubMed: 21998458]
26. Larocque D, Sanderson NS, Bergeron J, Curtin JF, Girton J, Wibowo M, et al. Exogenous fms-like tyrosine kinase 3 ligand overrides brain immune privilege and facilitates recognition of a neo-antigen without causing autoimmune neuropathology. Proc Natl Acad Sci U S A. 2010; 107:14443–8. [PubMed: 20660723]
27. Pellegatta S, Poliani PL, Stucchi E, Corno D, Colombo CA, Orzan F, et al. Intra-tumoral dendritic cells increase efficacy of peripheral vaccination by modulation of glioma microenvironment. Neuro Oncol. 2010; 12:377–88. [PubMed: 20308315]
28. Yamanaka R, Homma J, Yajima N, Tsuchiya N, Sano M, Kobayashi T, et al. Clinical Evaluation of Dendritic Cell Vaccination for Patients with Recurrent Glioma: Results of a Clinical Phase I/II Trial. Clinical Cancer Research. 2005; 11:4160–7. [PubMed: 15930352]
29. Liu Z, Davis C, Cai W, He L, Chen X, Dai H. Circulation and long-term fate of functionalized, biocompatible single-walled carbon nanotubes in mice probed by Raman spectroscopy. Proc Natl Acad Sci U S A. 2008; 105:1410–5. [PubMed: 18230737]

Statement of Translational Relevance

Immunotherapy is an attractive treatment modality for immunogenic tumors such as melanomas. However, frequent spread of these tumors to the brain, which is considered to be an “immune privileged” organ, may limit the clinical efficacy of this approach in some patients. Recently, while examining the role of CpG immunotherapy in experimental gliomas, we observed a systemic antitumor response following intracerebral delivery of CpG with carbon nanotubes (CNT-CpG). Here, we have confirmed these findings in a melanoma model by demonstrating that intracranial CNT-CpG therapy not only inhibited the growth of brain tumors, but also subcutaneous melanomas. To our knowledge, these results have not been previously reported and they suggest that intracerebral CNT-CpG therapy may have utility for the treatment of not only of gliomas, but also metastatic brain tumors.

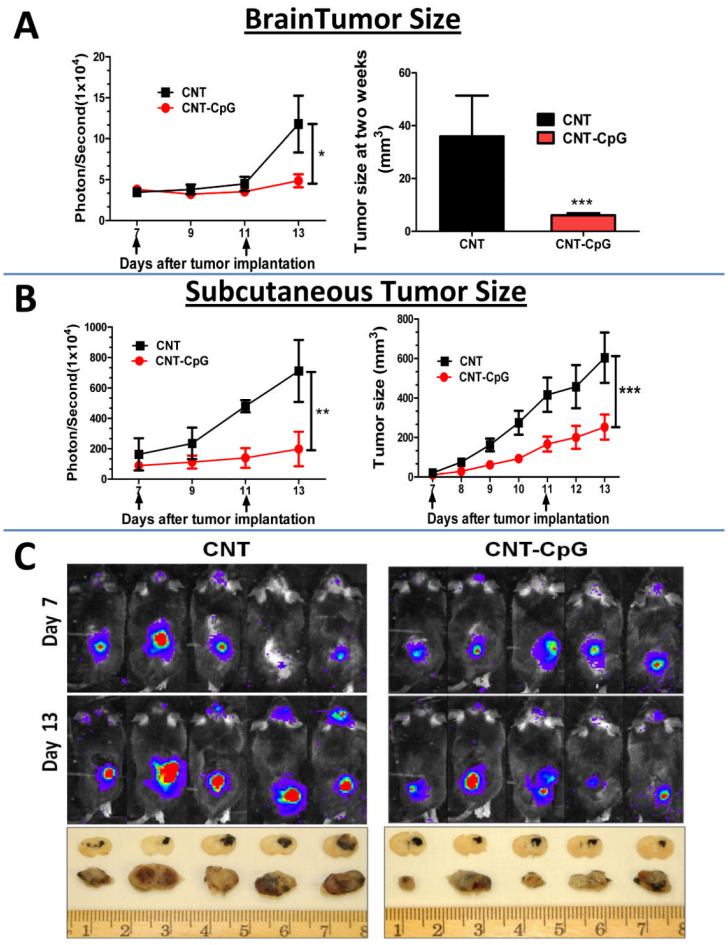

Figure 1.

CNT-CpG abrogates growth of melanomas following intracranial (i.c.) injection. Mice bearing both i.c. and subcutaneous (s.c.) B16.F10-luc melanomas were treated with i.c. intratumoral injections of either blank CNTs (2.5 μg) or CNT-CpG (2.5 μg CNT-5 μg CpG) 7 and 11 days (arrows) after initial tumor implantation. Tumor growth was evaluated by Xenogen (left graphs in A and B) and direct tumor size measurements with calipers (right graphs in A and B). Top panel C, Representative Xenogen images 7 and 13 days after tumor implantation; bottom panel C, brain and s.c. tumor cross sections 14 days after implantation illustrating the size of black-pigmented tumors. Data is representative of two separate experiments. n=5 mice/group, *: P< 0.05, **: P< 0.01, ***: P< 0.001.

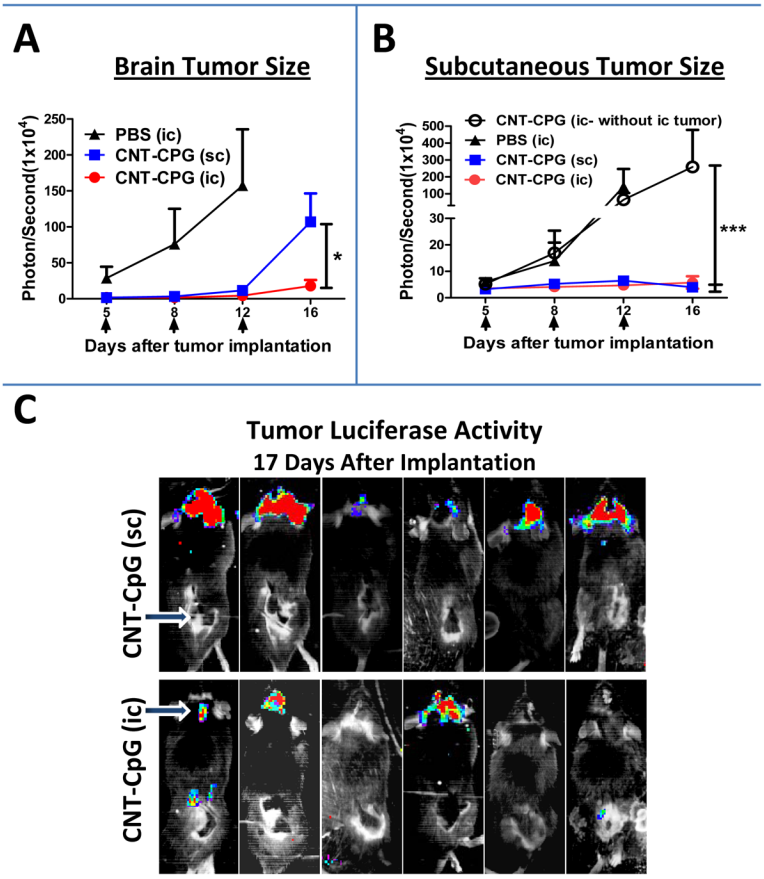

Figure 2.

Comparison of intracranial (i.c.) and subcutaneous (s.c.) CNT-CpG therapy in melanomas. Mice bearing both i.c. and s.c. B16.F10-luc melanomas were treated with either intratumoral i.c. PBS, i.c. CNT-CpG (2.5 μg CNT-5 μg CpG), or s.c. CNT-CpG (2.5 μg CNT-5 μg CpG) 5, 8, and 12 days after tumor implantation (arrows). Tumor growth was evaluated by Xenogen imaging. A and B, Intracranial CNT-CpG inhibited the growth of both i.c. and s.c tumors while s.c. CNT-CpG antitumor response was mostly local. Intracranial injection of CNT-CpG into mice bearing only s.c. tumors (open circles) has no systemic antitumor response (B). C, Representative Xenogen images of CNT-CpG-treated mice 17 days after tumor implantation. Arrows in C indicate site of CNT-CpG injections. Data is representative of two separate experiments. n=6 mice/group, *: P< 0.05, ***: P< 0.001.

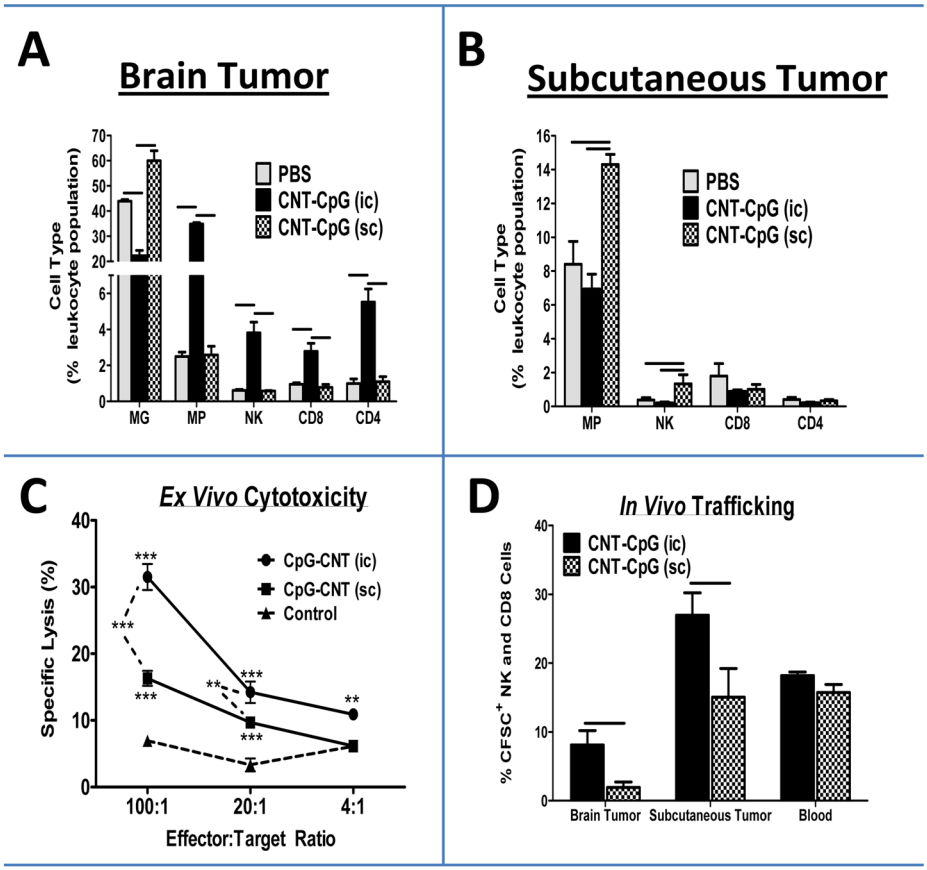

Figure 3.

Role of tumor microenvironment on CNT-CpG therapy. Mice bearing both intracranial (i.c.) and s.c. subcutaneous (s.c.) tumors were injected with CNT-CpG (2.5 μg CNT-5 μg CpG,) in either location four days after implantation. A and B, Proportion of tumor inflammatory cells was quantified by flow cytometry in both brain and s.c. tumors 24 hours after CNT-CpG injection. n=4 mice/group; C, *Ex vivo* cytotoxicity. Mice bearing either i.c. or s.c. tumors (n=4/group) were injected with intratumoral CNT-CpG four days after initial tumor implantation and every 3 days thereafter. Splenocytes were harvested 48 hours after the final treatment and examined for killing of B16.F10 target cells. Non-tumor bearing naive mice were used as controls. n=4 mice/group, D, *In vivo* leukocyte trafficking. Mice bearing either i.c. or s.c. tumors (n=3/group) were injected with intratumoral CNT-CpG four days after initial implantation and every 3 days thereafter. Splenocytes were isolated 24 hours after the third CNT-CpG injection, labeled with CFSE and re-injected into recipient mice (1×10^5 cells/mouse) bearing 10 day-old untreated i.c. and s.c. melanomas (n=5/group). Tumors and blood were harvested 24 hours later and tested for the presence of CFSE-labeled NK and CD8 cells by flow cytometry. *: P< 0.05, **: P< 0.01, ***: P< 0.001, Bars: P< 0.05.

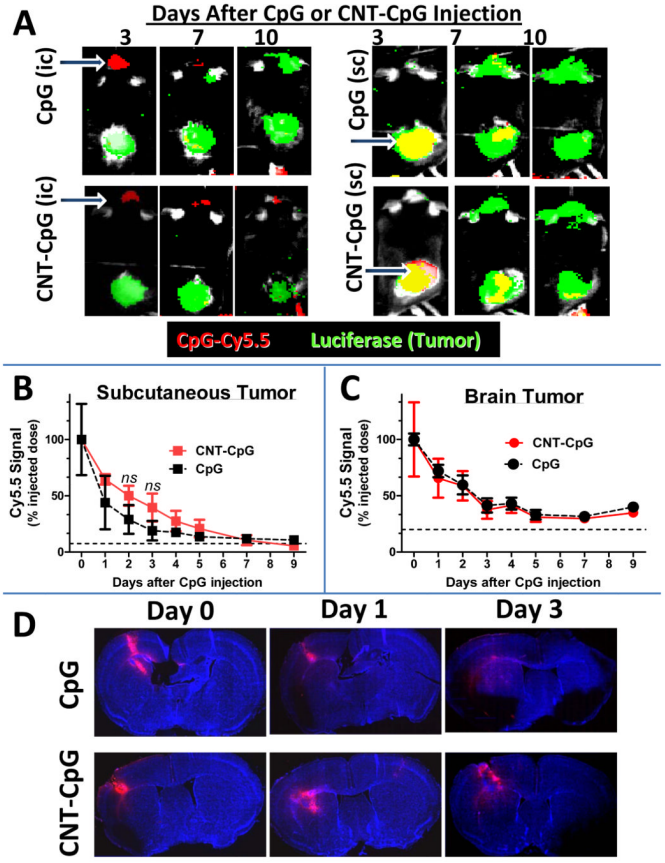

Figure 4.

CNT-CpG and CpG clearance in intracranial (i.c.) and subcutaneous (s.c.) melanomas. Mice bearing four day-old i.c. and s.c. B16.F10-luc melanomas (green) were injected intratumorally (indicated by arrows in A) with Cy5.5-labeled (red) CpG (A, top panel) or CNT-CpG (A, bottom panel). Tumor growth and Cy5.5 signal were measured by Xenogen (B and C). A, Representative mouse from each group demonstrating CNT-CpG and CpG clearance in relation to tumor growth. B and C, CpG and CNT-CpG clearance from s.c. and brain tumors. Data is representative of two separate experiments. Dashed lines represent background signal. n=6 mice/group. D, CNT-CpG and CpG distribution in i.c. tumors. Mice bearing four day-old melanomas were injected intratumorally with Cy5.5-labeled (red) CpG or CNT-CpG. At different time intervals brains were harvested, sectioned and imaged with fluorescent microscopy. CpG diffused away from the injection site, while CNT-CpG appeared to disperse around the tumor.

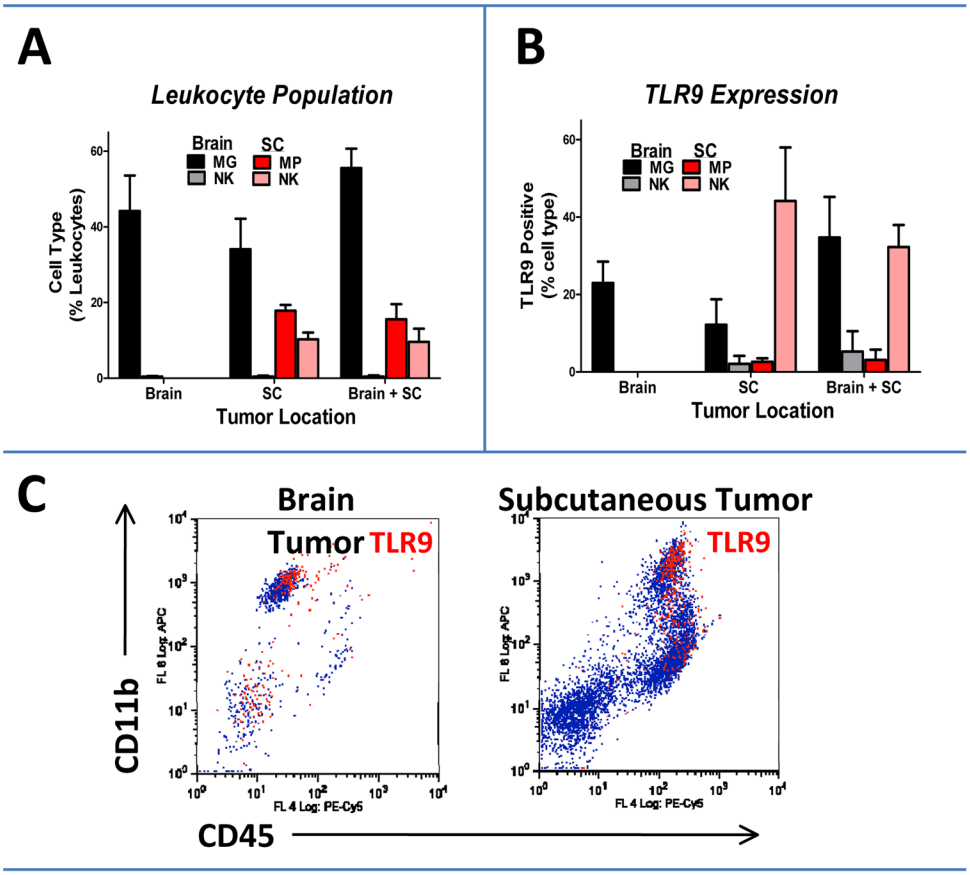

Figure 5.

Quantification of TLR9 expression in brain and subcutaneous (SC) melanomas. Seven days after tumor implantation, brain and SC tumors were assessed for leukocyte infiltration (A) and TLR9 expression (B) by flow cytometry. C, Representative dot plots of tumor-associated macrophages (MP, $CD45^{high}$ $CD11b^{+}$) showing TLR9 expressing cells as red events. Microglia (MG: $CD45^{low}$ $CD11b^{+}$) were the most common $TLR9^{+}$ cells in brain tumors. Data is representative of two separate experiments. n=4 mice/group.

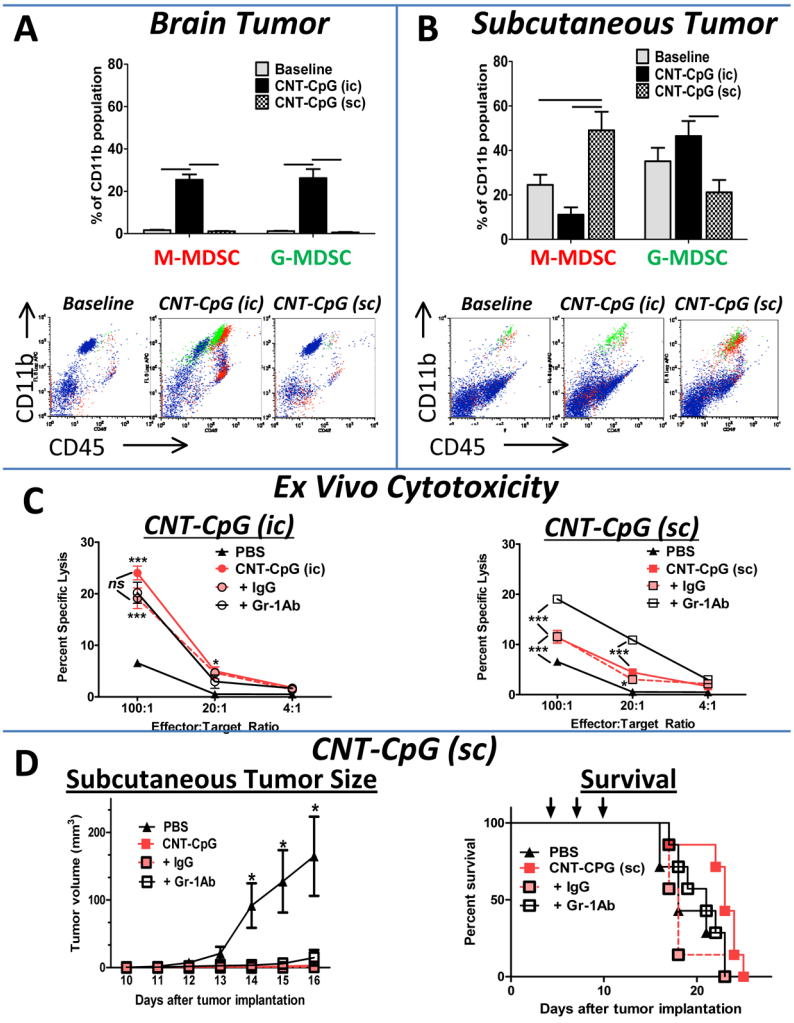

Figure 6.

Role of myeloid-derived suppressive cells (MDSC) in CNT-CpG therapy. A and B, Quantification of MDSC. Mice bearing both intracranial (i.c.) and subcutaneous (s.c.) tumors were injected with i.c. PBS (baseline), i.c., or s.c. CNT-CpG four days after tumor implantation. Proportion of MDSC was quantified by flow cytometry in both brain (A) and s.c. (B) tumors 24 hours after CNT-CpG injection. Monocytic MDSC (M-MDSC; Ly6C^{high}) and granulocytic MDSC (G-MDSC; Ly6G^{high}) are shown as red and green events, respectively, in representative dot plots. n=4 mice/group. C and D, Impact of Gr-1 depletion on CNT-CpG antitumor response. Mice were treated with anti-Gr-1 mAb or control IgG one day prior and every 3 days after tumor implantation. A, Mice (n=4) bearing four day-old i.c. and s.c. tumors were treated with intratumoral PBS or CNT-CpG (three injections as in Fig 3C), splenocytes were harvested 48 hours later and examined for killing of B16.F10 target cells. D, Antitumor response was measured in mice bearing both i.c. and s.c. tumors treated only with s.c. CNT-CpG four, seven and ten days (arrows) after tumor implantation. n=7 mice/group. Data is representative of two separate experiments, bars and *: P< 0.05, **: P< 0.01, ***: P< 0.001.